

# Synergies and Exploratory Procedures for Haptic Object Recognition

Author1, Author2, ..., AuthorN

May 2024

## Abstract

The purpose of this article is to study the role that synergies play in the characterization of movements and exploratory procedures we perform while exploring different objects through touch. These synergies have been proposed as a good tool for describing such movements as well as the method used by the central nervous system to control the high-dimensional space of the hand. We will analyze if this approach provides an advantage in describing the exploratory procedures and the hand movements in an open exploration of an object. We will also create different mathematical/machine learning-deep learning models to study exploratory procedures and their relationship with certain physical characteristics of the objects to be explored. Finally, the results of different classification methods present in the literature are analyzed and discussed to elucidate the advantages and disadvantages that each of them presents.

## Keywords

Active Object Exploration, Exploratory Procedures, Postural Synergies

## Background and motivation

An overview of the study design, the assay(s) performed, and the created data, including any background information needed to put this study in the context of previous work and the literature

- experiment from Lederman & Klatzky: three objects belonging to a common object family with two being a variation of each other and one being further apart (Drinking vessels: ceramic cup, metal cup, glass), to the subject one out of three objects from a object family is handed over together with naming one out of the same three objects. In one of three cases, the

given and the named object are the same, in the two other cases they differ. The participant is asked to answer as fast as possible with 'yes' when the given and named object match and with 'no' otherwise (two-choice alternative task).

- first finding: object properties are extracted using stereotypical repetitive motion patterns: the exploratory procedures (EPs) [ref: first study]
- second finding: according to Lederman & Klatzky human use the most discriminative attribute (MDA) to discriminate between two possible objects
- multi-modal: kinematic data of upper body and right arm + first finger joint (joint angles) from optical tracking and first second and third joint from sensorized glove, high density EMG on the forearm (64 electrodes) and bi-polar EMG on the upper arm and shoulder (6 electrodes?), tactile interaction right hand (58 sensors)
- timestamped EP labels
- 3D models of objects used in the dataset
- given and asked object as well as given answer (binary)

broader goals that motivated the creation of this dataset and the potential reuse value:

- EPs only described qualitatively, no quantitative data given
- dataset can enable creation of EP descriptors (possible: kinematic synergies)
- develop models for object discrimination/recreation from kinematic-tactile perception
- 

## Classification by Raw Data

The idea is to build different classifiers (logistic regression and time-series) using the raw data from the different sources that we have, compare their performances and check which is the most adequate methodology to apply.

### Methods:

- Build a logistic regression classifier and a time-series DL based classifier using each source (motion tracking, EMG & tactile) and compare results.

- For the logistic regression classifiers, extract and study the most relevant variables and if their weight difference is significant or not (between variables inside the same family, between families, ...). Since we have very few trials per subject, comparing between subjects might not be useful.
- Study weight evolution over time.
- Build logistic regression and time-series classifiers from the combination of sources, compare results between combinations and methods (multisource vs. hierarchical) and study if accuracy differences are significant.
- It can be interesting to compare the raw EMG with the same classifier but based in feature extraction as in *Leo et al.* [1] both in logistic regression and time-series classifiers.
- It can be interesting to compare raw single source vs. normalized single source.
- It can be very interesting to explore early enclosure classification with raw kinematics and EMG (as in *Scano et al.*) [2].

## Expected results & discussion:

For the logistic regression classifiers, preliminary results (with trials divided into EPs) show poor ( $\sim 50\%$ ) but above chance classification accuracies for within-group classification. Time-series classifiers perform very good for within-group but not when we try to classify among all objects. Hierarchical classifiers seems to be a little better than single-source or multimodal classifiers for logistic regression. The hierarchical approach has not been tested yet on time-series classifiers but the multimodal classifier outperforms the single-source. Tactile data seems to confound the classifier. Although this section does not present any significant advances in this research field, both the complexity of the experimental task and the methodological issues addressed in it do represent a considerable novelty. If we perform also classification based on early enclosure we can compare to all those synergy studies based on reach & grasp or virtual grasping and overcome the problem with the difference in trial lengths.

## Synergies

Synergies were defined by Bernstein in 1967 [3] and proposed as an interesting way to describe and characterise hand movements on a kinematic and muscular level [4]. *Thakur et al.* thought of synergies as "building blocks of EPs" [5]. They have also been proposed as the basic patterns used by the CNS to control hand postures [6]. The purpose of this section is to find these synergies and see if they can be used as a good descriptor of hand movements even for more complex tasks like ours. We also want to study if those synergies are shared between subjects and tasks and if they constitute "the building blocks" of EPs.

In this section we will be using again the logistic regression and the time-series classifiers.

### Methods:

- Extract synergies using different methods for each source (PCA for kinematics, NMF for EMG, ...).
- Study if these synergies are shared between subjects, objects, families, trials, EPs, ...
- Classify objects based on those extracted synergies and compare it with previous classifiers with raw data (including multisource and hierarchical).
- Study how the classification accuracy decays as we drop synergies.
- For the EMG, extract the synergies not from the raw data but from the EMG features (as in *Leo et al.* [1]) and then classify. Compare that classifier with the previous classifiers from EMG data.
- Compare the most relevant variables in the most relevant synergies with the variable weights in previous classifiers.
- Compare different methodologies when extracting the synergies (normalize or not, extract synergies from each subject and build clusters or extract synergies from the entire dataset) as mentioned in *Gracia-Ibañez et al.* [7].
- Extract synergies from early enclosure and build classifiers using them using them. Compare the obtained synergies between subjects, objects, families, ...

### Expected results & discussion:

We expect to find that the precision remains at acceptable levels even after considerably reducing the dimensionality of the problem. Preliminary results show that synergy patterns are not shared among EPs, objects or subjects. This section can give us some ideas of how this method based on synergies behaves in more complex tasks, providing evidence about its possible utility or application. In case synergies are good describers for early enclosure (se seen in literature) but the number of synergies necessary to describe the entire trial is close to the number of dimensions in the original space, it could be argued that this approach is only a "mathematical artifact" and would not have any advantage for the CNS when it comes to controlling the motor system in general and the hand movements in particular.

## Classification by EPs used

The intention is to build classifiers based on the EPs performed by the subject during the exploratory task. These three classifiers would be based on presence/absence, the number of occurrences and the time duration of the EPs. The internal weights of that classifiers would give us an idea of which EPs are most relevant. Since each EP is associated with some physical properties we want to connect the most relevant EPs with those physical properties that are relevant to discriminate the objects.

### Methods:

- Build three different logistic regression classifiers (binary, count, execution time) to predict the object within the family and the same three classifiers to predict among families.
- Extract and analyse the model weights to find the EPs that the model considers relevant. Study if weight difference is significant or not (between variables inside the same family, between families, ...). Again, since we have very few trials per subject, comparing between subjects might not be useful.
- Compare results and weights between classifiers.
- Compare the properties associated to the most relevant EPs for each object and family with the physical property that discriminates those objects the most.
- Compare results with those presented by *Lederman & Klatzky* [8, 9].

### Expected results & discussion:

We have some preliminary results that supports the findings presented by *Lederman & Klatzky* [8, 9]. Even though these results are not very solid (classification accuracy is low but above chance level) we can present this as a "quantitative" approach to their work and new evidence in favour of their hypotheses.

## 1 Methods

### Participants

Ten healthy individuals (4 females, 6 males), aged 24 to 36 (mean age:  $30.3 \pm 4.0$  years, weight:  $69.5 \pm 15.4$  kg, height:  $172.4 \pm 8.0$  cm), all right-handed and without known neuromuscular impairments, participated. Participants provided written consent before data collection. Experiments adhered to the Declaration of Helsinki and were approved by the local ethical committee (CER Liguria Ref. 11554, October 18, 2021).

## Experimental setup and data acquisition

Kinematic data was recorded two fold. On the one hand using MoCap (Vicon) and on the other hand using a sensorized glove from CyberGlove (CyberGlove I). Vicon Nexus software extracted anatomical joint angles from marker trajectories, utilizing Plug-in Gait and RHand Bodybuilder models for torso, upper-arm and finger joints, respectively. Signals are sampled at 100 Hz. Data included MCP joint angles for all fingers and STT joint angle for the thumb. CyberGlove tracks finger joints (MCP, PIP) and thumb movements. Wrist motions are also recorded, with Pitch indicating flexion/extension and Yaw indicating radial/ulnar deviation. Joint angles are inferred from sensor deformation, requiring individual calibration per user. The offline calibration process is described in the sup. mat.

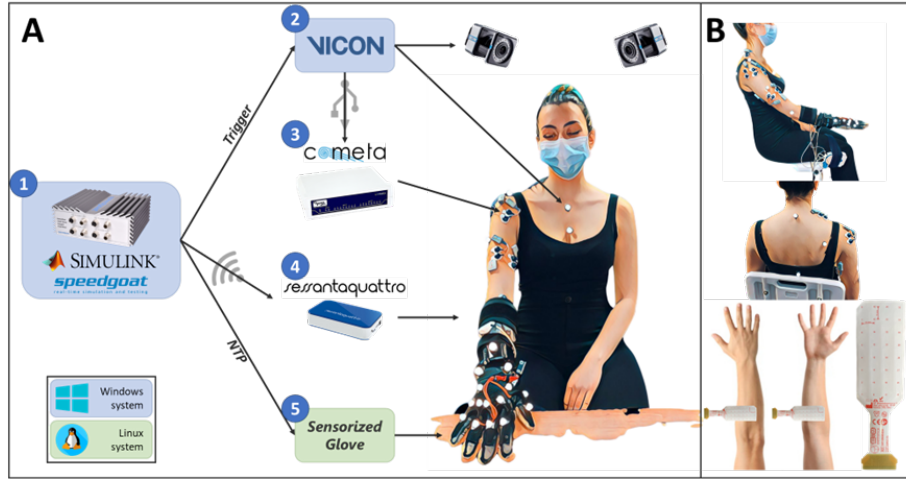


Figure 1: Experimental setup. A: 1) Real Time target machine Speedgoat running the Simulink model. 2) Vicon motion capture system. 3) Cometa system bipolar EMG. 4) Sessantaquattro high-density EMG. 5) Sensorized glove from Bielefeld University. B: Placement of the acquisition sensors: 23 reflective markers for the Vicon system, 10 bipolar EMG electrodes, 2 grids for HD-sEMG acquisition, and sensorized glove.

Tactile data, obtained through soft piezoresistive pressure sensors developed by Bielefeld University for the WearHap EU-project, lacks absolute calibration but enables relative comparisons. These sensors, integrated on palm and finger interiors, measure pressure applied over time, aiding in analyzing force distribution during manipulation. The glove hosts 58 taxels, with 17 on the palm and the remainder distributed across fingers.

HD-sEMG data was recorded using the Sessantaquattro device with two grids of 32 electrodes each placed over the flexor and extensor muscle of the forearm. Bipolar EMG was wirelessly collected from the Upper Trapezius, An-

terior Deltoid, Middle Deltoid, Posterior Deltoid, Long Head of Biceps, Short Head of Biceps, Lateral Head of Triceps, Medial Head of Triceps, Brachioradialis, and Pronator Teres using the Wave Plus system. Data is sampled at 2 kHz.

More detailed information can be found in the sup. mat.

## Experimental protocol

First the participant was provided with the aim of the experiment, the experimental procedure and the setup. Before the experiment the subjects could visually familiarize with the object families and their members. After that, the sensor equipment was attached and the participant took place on a chair and set comfortable. The sight was blocked to prevent visual clues and the ears were covered with active noise canceling headphones to prevent auditory cues. The participant were instructed to answer correct as fast as possible by only using haptic object exploration with their right hand exclusively. The order of questions is randomized per participant. The experimenter would reach to the participant the object to explore alongside the question, after confirming the readiness.

For example:

Experimenter: "Are you ready?"

Participant: "Yes."

E: "Is the object I hand to you a ceramic cup (while handing over a glass)?"

P: performs haptic object exploration.

P: "No."

The subject would get no feedback on their performance before the end of the experiment. At the end the participants were asked about there experience and how difficulty they rate the task. The experiment contained 5 object families with 3 objects each and a total of 45 trials. It lasted approximately 1 hour in total. After each task, participants rested for at least 20 seconds to prevent fatigue.

## 1.1 Synergy extraction, mapping, and clustering

There is evidence, that synergies are shared between subjects and they carry task specific information across subjects. Can also exploratory procedures (EPs) be explained by synergies? To study the similarity between different subjects and EPs a process including synergy extraction, mapping and clustering is proposed. Synergies are extracted for each objective (subject or EP) in Sec. 1.1.1 and using element wise matching of the loadings (joint recruitment) of each synergy (Principal Component (PC)) the overall similarity of the pair is calculated, Sec. 1.1.2. In Sec. 1.1.3 we group synergies using clustering algorithms. [additional study in Sec. 1.2]

### 1.1.1 Synergy extraction

The data is split according to the objective under study (subject or EP) into subsets. On each subset Principal Component Analysis (PCA) is applied explaining  $\geq 95\%$  of the variance and deriving a set of synergies per objective.

Initial data analysis reveals, that some PCs have inverted loadings where the loadings are flipped along the x-axis ( $PC_x = (-1) \cdot PC_y$ ). In practical terms: The joint recruitment follows an identical distribution, but the generated motion has the opposite direction (hand opening vs. hand closing, same joint recruitment distribution with different direction). We consider this as an optimal match, based on a semantic and not neuronal reasoning. Additionally we used further distance metrics without the mentioned consideration. Namely: cityblock distance and euclidean distance. Synergies are expressed by:

$$\mathbb{X} = \mathbb{Z}\mathbb{Y}^T \quad (1)$$

with the matrix  $\mathbb{X}$  being the time series data of the dimension (*samples*  $\times$  *nb\_joints*),  $\mathbb{Y}$  being the loadings of the dimension (*principalcomponents*  $\times$  *nb\_joints*) and  $\mathbb{Z}$  being the PCs of the dimension (*samples*  $\times$  *principalcomponents*). The data in the lower dimensional space  $\mathbb{Z}$  is found by  $\mathbb{X}\mathbb{Y}$ .

### 1.1.2 Synergy mapping

Once the synergies per objective are extracted a pairwise comparison is performed. For the pairwise comparison correlation and two distance metrics are used (cityblock and euclidean distance). With that a correlation or distance value for each PC is extracted allowing to find the nearest neighbor/best match. [Using pairwise comparison has the benefit to allow different number of synergies to be compared.]

The mapping can be visualized on a 2d graph spanning over the PCs of two objectives (e.g. subject1 and subject2). Given the first PC of the first objective matches best with the first PC of the second objective and so on will lead to all entries lying on the diagonal of the 2d graph, or almost on the diagonal for unequal amount of synergies. The further entries are diverging from the diagonal, the worse is the match. calculating the mean distance over the distance from all points to the optimal diagonal gives us a single value similarity score for each compared pair. The score is normalized by the number of PC used. This allows using the mapped synergies as distance metric.

### 1.1.3 Synergy clustering

All the derived distances can be visualized in a heatmap and be used to cluster the single objectives into groups by the mean of hierarchical or kmeans clustering. For the first case the number of clusters is derived from the hierarchical clustering algorithm using different objectives (Single Linkage, Complete Linkage, Average Linkage, Ward's Method). For the second case the silhouette score is calculated first to find the best number of clusters followed by kmeans clustering.



## 1.2 Linear combination

After extracting all synergies per objective, we validate how many fix base sets are sufficient to explain the pool of PCs. Finding the base sets is a non-trivial optimization problem which is unsolvable by gradient descent methods. Optimization based on a Genetic Algorithm (GA) was deployed instead to create the base sets using the Python library PyGAD [10]. To find the optimal weight (Eq. 2) for each member of the pool and the weighted sum of the base sets we deployed the minimize function from the scikit-learn library.

$$\begin{aligned} \vec{y}_{lc}(S) &= \sum_{n=1}^N \alpha(N) \vec{y}_{bs}(N) \\ \text{minimize } error(S) &= |\vec{y}(S) - \vec{y}_{lc}(S)| \end{aligned} \quad (2)$$

with  $\vec{y}$  being the loadings of a single PC (of the dimension *nb\_joints*) and the subscript *lc* stands for *linear combination*, the subscript *bs* for *base set*, and the synergy under study out of the pool is denoted by  $S$ . The number of base sets is denoted by  $N$ . Note that each PC with its *nb\_joints* members has its own shared weight  $\alpha(N)$ . In other words: every member of the base set vector  $\vec{y}_{bs}$  has exactly one  $\alpha$  assigned to it.

The fitness function of the GA is defined as the inverse of the sum of the mean pairwise error over all loadings and all members of the pool as following:

$$\begin{aligned} fitness &= error^{-1} \\ error &= \sum_{l=1}^L \left| \frac{\sum_{m=1}^M y_{lc}(m) - y(m)}{M} \right| \end{aligned} \quad (3)$$

with  $L$  being the number of extracted PCs (e.g pool size) and  $M$  the number of joints in the original data.

The optimization starts with a single base set and iteratively increases the number of base sets when the maximum number of generations are computed, or no improvement is noted after 5 generations. The process is repeated until  $\frac{L}{2}$  generations are reached, or the *error* falls below 1e-3.

## 2 Results

### 2.1 Synergy extraction

#### 2.1.1 Subject

For [n] subjects 12 synergies have been extracted, for the remaining [m-n] 13 synergies. Only to explain 95% of all data 14 synergies were necessary. To test how much the synergies of a given subject generalize the reconstruction error was calculated. The mean reconstruction error is  $(x \pm y)^\circ$  which leads to the conclusion that the synergy sets are [very similar/same descriptive power?]. Nonetheless are differences notable. The synergies of subject 2 have the heighest

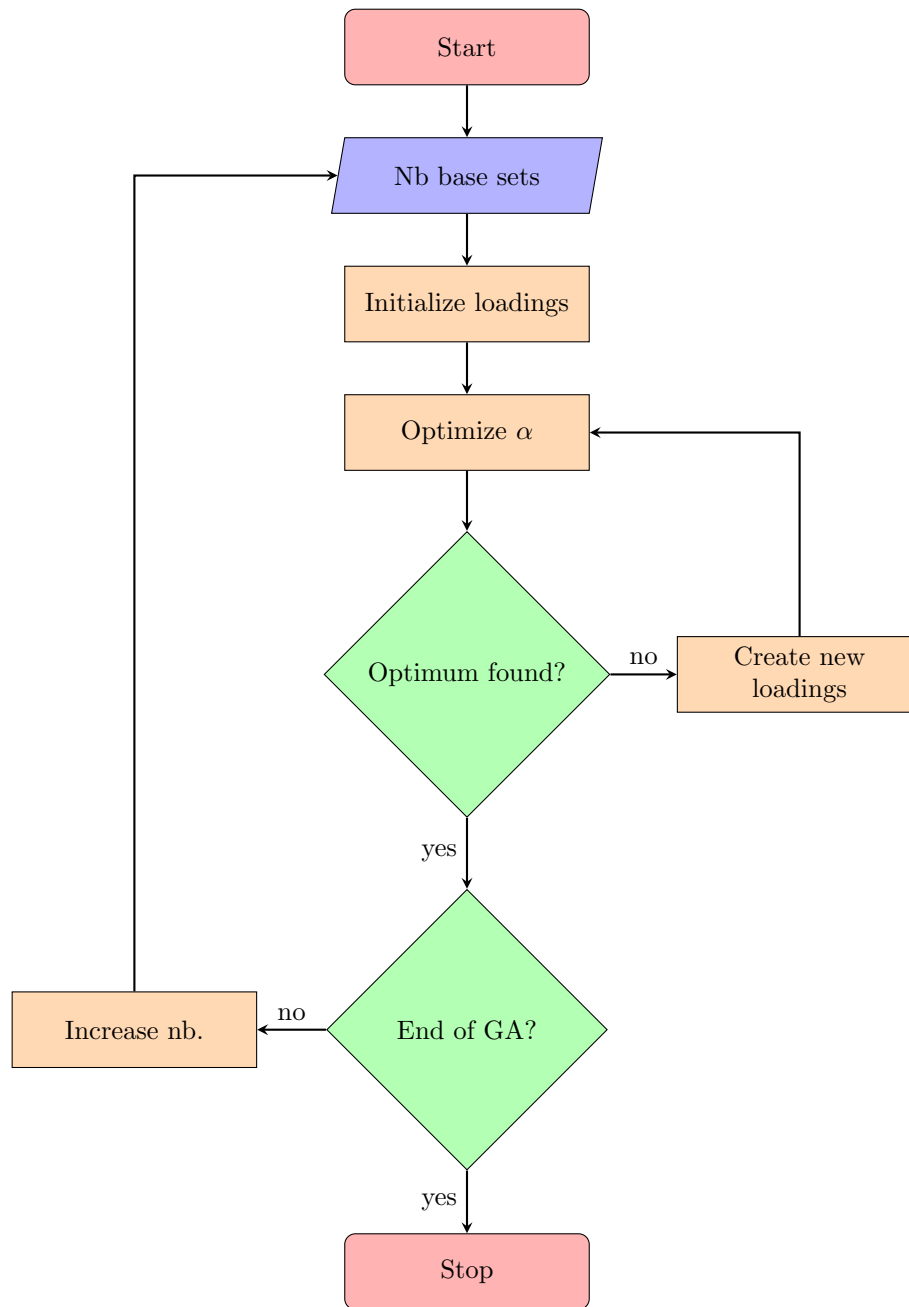


Figure 2: Shows the workflow of the genetic optimization to find the number of base sets required to reproduce all found synergies.

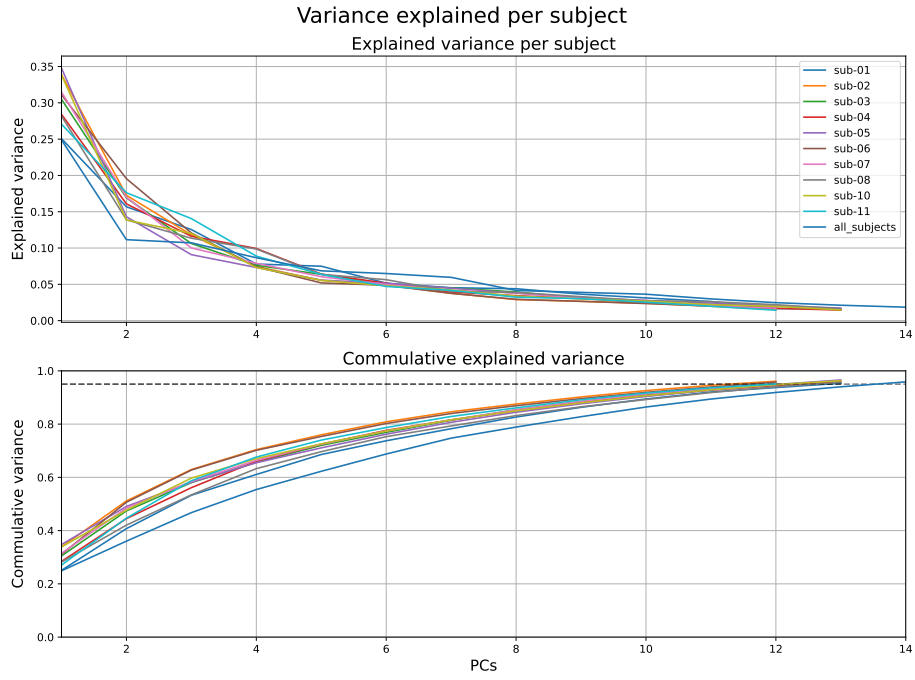


Figure 3: Number of extracted synergies per subject (including all subjects) to reach 95% explained variance.

error when encoding data from different subjects with  $(x \pm y)^\circ$  [look at number datapoints=exploration time] whereas its data can be explained best by other synergies with  $(x \pm y)^\circ$ .

### 2.1.2 Exploratory procedures

### 2.1.3 Synergy mapping

#### Subject

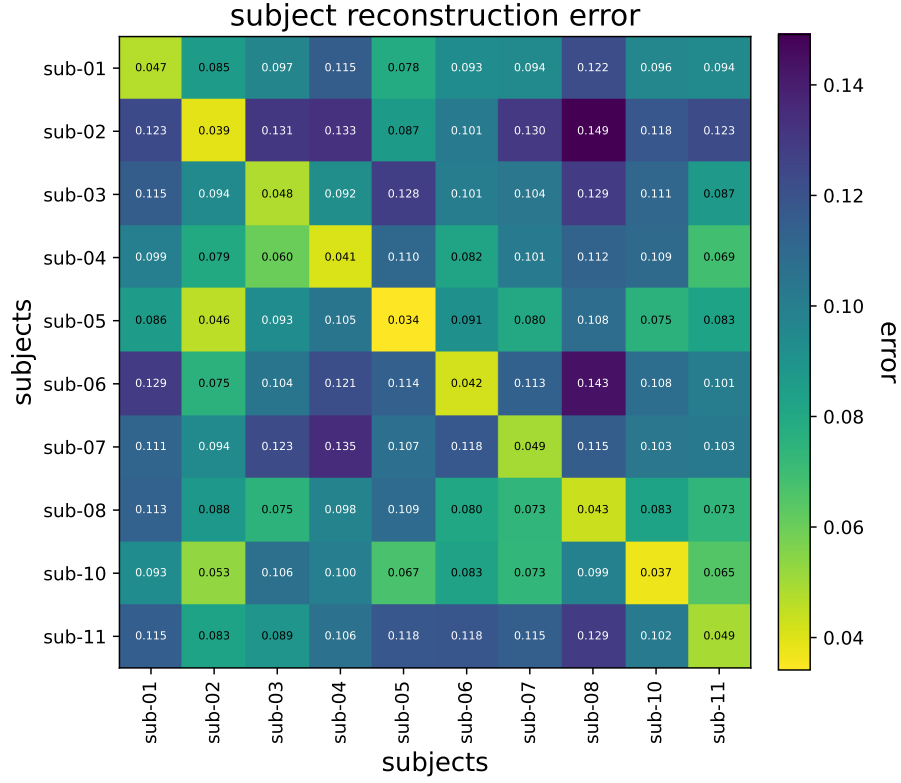


Figure 4: The reconstruction error from each model applied to all data splits.

#### 2.1.4 Exploratory procedures

### 2.2 Synergy clustering

#### 2.2.1 Subject

#### 2.2.2 Exploratory procedures

### 2.3 Reconstruction Error and explained variance ratio

#### 2.3.1 Subject

#### 2.3.2 Exploratory procedures

### 2.4 Linear combination

#### 2.4.1 Subject

#### 2.4.2 Exploratory procedures

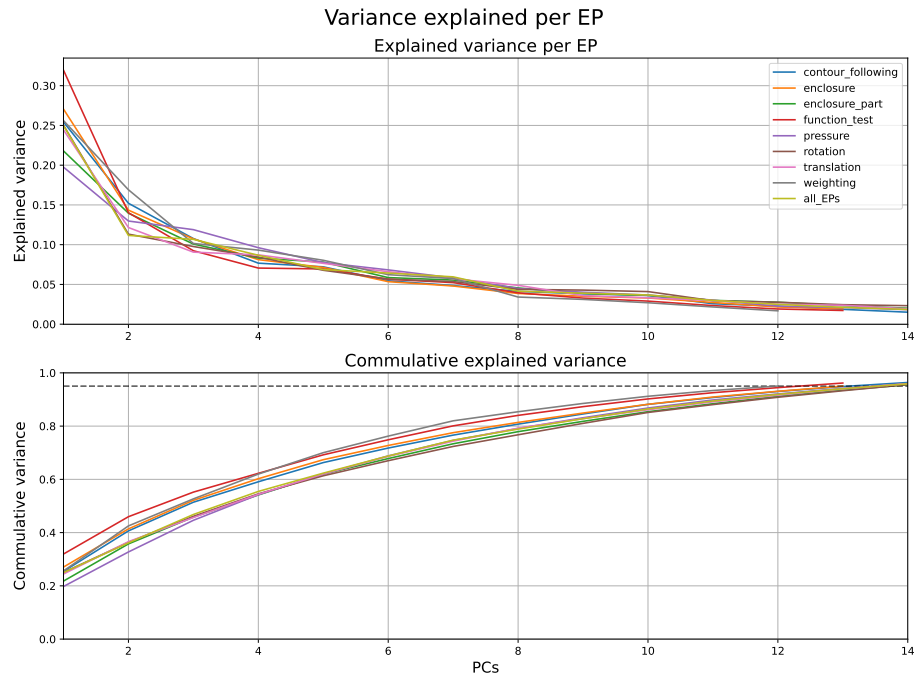


Figure 5: Number of extracted synergies per subject (including all subjects) to reach 95% explained variance.

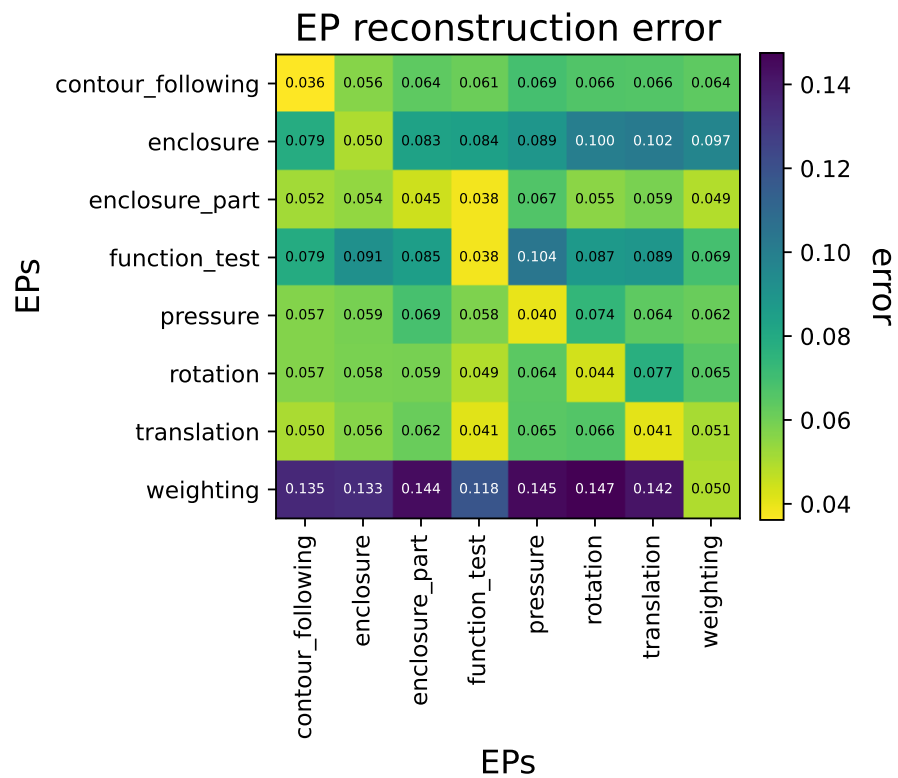


Figure 6: The reconstruction error from each model applied to all data splits.

Supplementary material

Author1, Author2, ..., AuthorN

May 2024

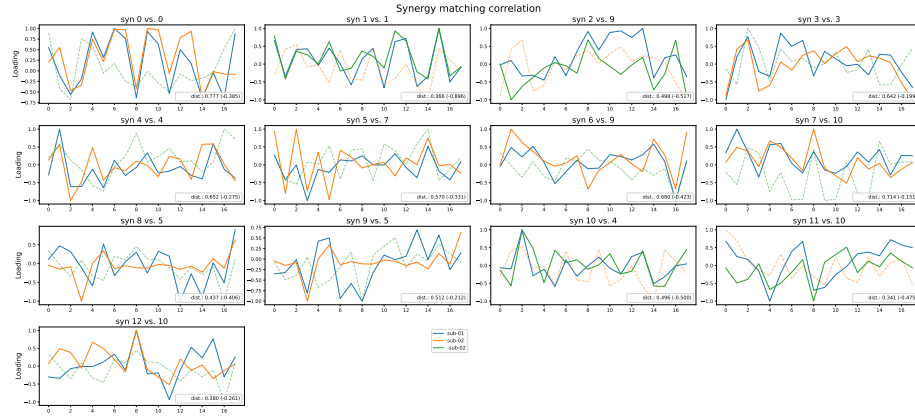
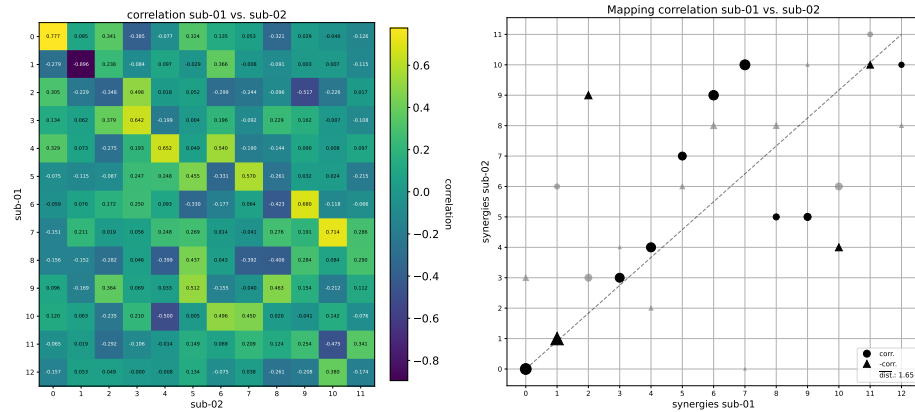


Figure 7: The result of the mapping of the synergies of subject 2 on the synergies of subject 1. The synergies of subject 2 which have the highest (lowest) correlation are mapped and visualized together. Correlation allows to detect anti-correlated pairs which are shown in green.



(a) Shows the correlation between every synergy of subject 1 with every synergy of subject 2. (b) Number of extracted synergies per subject (including all subjects) to reach 95% explained variance.

Figure 8: Similarity calculated using three different metrics.

## Participants

Ten healthy individuals (4 females, 6 males), aged 24 to 36 (mean age:  $30.3 \pm 4.0$  years, weight:  $69.5 \pm 15.4$  kg, height:  $172.4 \pm 8.0$  cm), all right-handed and without known neuromuscular impairments, participated. Participants provided written consent before data collection. Experiments adhered to the Declaration of Helsinki and were approved by the local ethical committee (CER Liguria Ref.

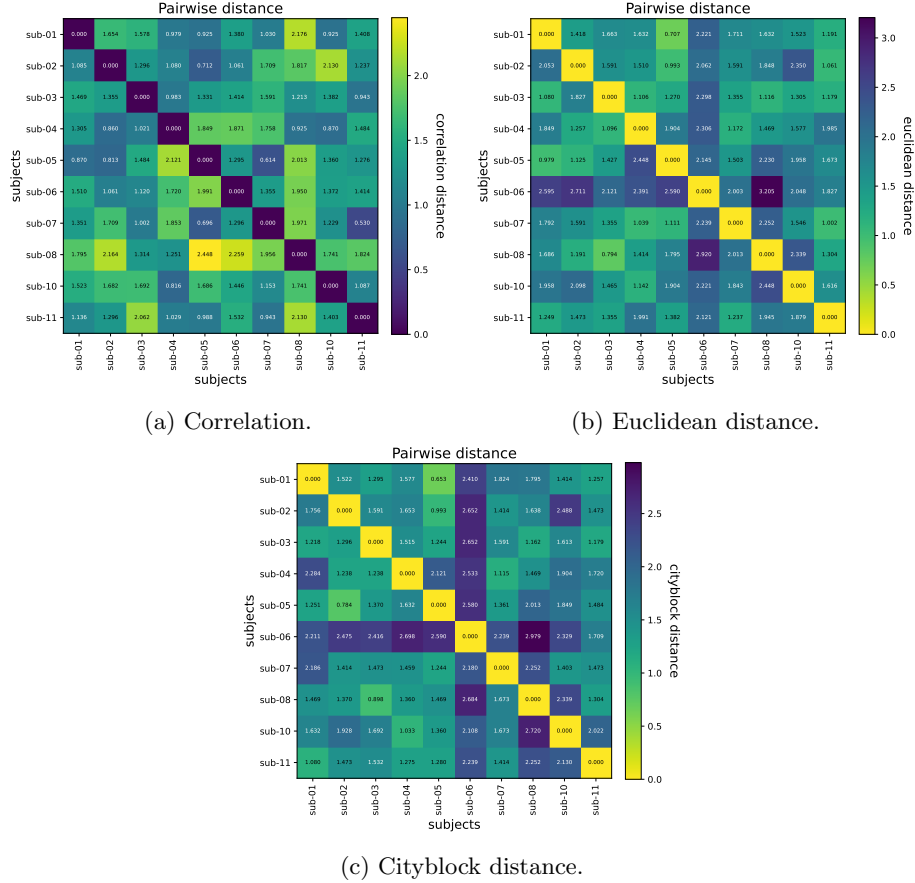


Figure 9: Similarity calculated using three different metrics.

11554, October 18, 2021).

## Setup and data acquisition

HD-sEMG data was recorded using the Sessantaquattro device with two grids of 32 electrodes each. The first grid was placed over flexor muscles (electrodes 1-32), while the second was placed over extensor muscles (electrodes 33-64). Electrodes were attached 5 cm below the olecranon. The reference electrode was on the ulnar styloid process. The device was fixed to the subject's leg. Data was sampled at 2 kHz with 16-bit resolution and a range of 18.75 mV peak to peak. A first-order high-pass filter removed the DC component at 10.5 Hz. See Supplementary Table for channel details and placements.

Bipolar EMG was wirelessly collected using the Wave Plus system (Cometa, Fig. 1.A.3). Myoelectric activity was measured via 10 bipolar pre-gelled adhe-



Table 1: HD-EMG channels numbers, abbreviations, and description of the physical placement.

HD-EMG channel	Abbreviation	Description
1	flexion_01	Distal flexor muscle
...	...	...
32	flexion_32	Distal flexor muscle
33	extension_01	Distal extensor muscle
...	...	...
64	extension_32	Distal extensor muscle

Table 2: Bipolar EMG channels numbers, abbreviations, and description of the physical placement.

EMG channel	Abbreviation	Description
1	Lat_Tric	Lateral Head of Triceps
2	Med_Tric	Medial head of Triceps
3	Long_Bic	Long Head of Biceps
4	Short_Bic	Short Head of Biceps
5	Ant_Delt	Anterior Deltoid
6	Midd_Delt	Middle Deltoid
7	Post_Delt	Posterior Deltoid
8	Upper_Trap	Upper Trapezius
9	Brachiorad	Brachioradialis
10	W_pronator	Pronator Teres

sive electrodes placed on specific muscles: Upper Trapezius, Anterior Deltoid, Middle Deltoid, Posterior Deltoid, Long Head of Biceps, Short Head of Biceps, Lateral Head of Triceps, Medial Head of Triceps, Brachioradialis, and Pronator Teres. Data was sampled at 2 kHz, with 16-bit resolution and a full-scale input range of 5 mV peak to peak. The DC component was filtered out internally using a first-order high-pass filter with a 10 Hz cut-off frequency. Supplementary Table 2 provides channel numbers, abbreviations, and descriptions of the physical placements of the bipolar EMG electrodes. The Wave Plus system connected to the PC running Vicon Nexus synchronized data from the Cometa (bipolar EMG) device with kinematics data from the Vicon system. Kinematic data, captured by MoCap (Vicon), used 10 infrared cameras and 23 reflective markers. Reflective markers were placed on bony prominences of the shoulder, elbow, wrist, knuckles, and phalanges, following Vicon’s Plug-in Gait and RHand models. Signals were sampled at 100Hz. Vicon Nexus software extracted anatomical joint angles from marker trajectories, utilizing Plug-in Gait and RHand Bodybuilder models for upper-arm and finger joints, respectively. Each joint’s rotations around Cartesian axes were described. The RHand Bodybuilder model computed joint angles for the right hand and fingers, providing both absolute and projected angles. Absolute angles were based on single vec-

tor representations, while projected angles represented flexion/extension and abduction/adduction of the metacarpophalangeal joint. Data included MCP joint angles for all fingers and STT joint angle for the thumb. We utilized a sensor-equipped glove developed by Bielefeld University (Figure 2) to capture finger movements (kinematic data) and grasping forces (tactile data). This glove, dubbed "cyberglove" for kinematic data and "tactileglove" for touch data, interfaces with a Linux OS (Ubuntu 20.04) via ROS Melodic, sampled at 100 Hz. ROS streamlines communication in robotics, including sensor data transfer.

Kinematic data, captured by the unaltered CyberGlove I from CyberGlove Systems, tracks finger joints (MCP, PIP) and thumb movements. Wrist motions are also recorded, with Pitch indicating flexion/extension and Yaw indicating radial/ulnar deviation. Joint angles are inferred from sensor deformation, requiring individual calibration per user.

Tactile data, obtained through soft piezoresistive pressure sensors developed by Bielefeld University for the WearHap EU-project, lacks absolute calibration but enables relative comparisons. These sensors, integrated on palm and finger interiors, measure pressure applied over time, aiding in analyzing force distribution during manipulation. The glove hosts 58 taxels, with 17 on the palm and the remainder distributed across fingers. However, taxels at the tip of the ring fingers were excluded due to hardware issues (Figure 9).

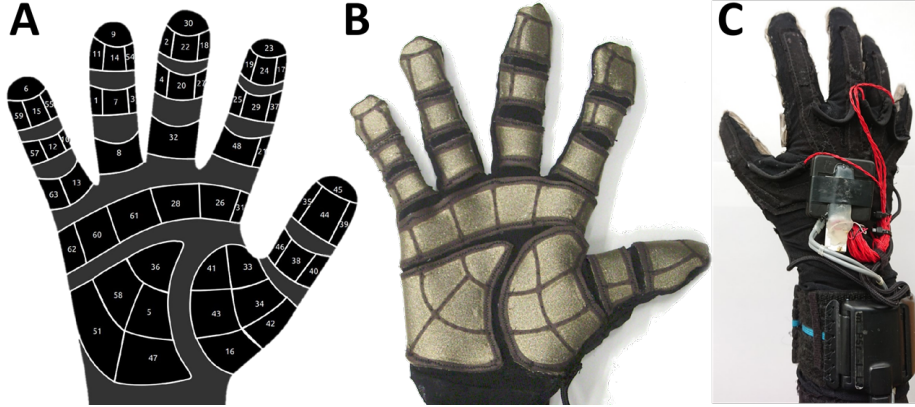


Figure 10: Sensorized glove. A: schematic representation of the taxels (tactile pixels) and the corresponding numbers. B: Front view of the glove palm with its 58 taxels. C: Back view of the glove with the embedded electronics.

Data acquisition required three computers. The ROS infrastructure for the tactile glove ran on a dedicated Linux machine. Two Windows machines were used: one for MoCap software and the other for a custom Matlab GUI to stream data from the Sessantaquattro system and for time synchronization among devices. The Simulink model for time synchronization and HD-sEMG recordings ran on a Real-Time Target machine, facilitating synchronization among all devices using a hardware voltage trigger signal. Additionally, Network Time Pro-

Table 3: Anatomical joints’ numbers, abbreviations, description of the movements.

Joint	Abbreviation	Description	
1	LThorax	Left thorax	X: Backward tilt Y: Right tilt Z: Right rotation
2	RElbow	Right elbow	X: Flexion-Extension Y: - Z: -
3	RShoulder	Right shoulder	X: Flexion-Extension Y: Abduction Z: Internal rotation
4	RThorax	Right thorax	X: Backward tilt Y: Left tilt Z: Left rotation
5	RWrist	Rigth wrist	X: Ulnar Deviation Y: Flexion-Extension Z: Pronation-Supination
6	RIndexJ1	Right index	Abs_X: Flexion-Extension Proj_Y: Flexion-Extension Proj_Z: Adduction-Abduction
7	RPinkieJ1	RightPinkie	Abs_X: Flexion-Extension Proj_Y: Flexion-Extension Proj_Z: Adduction-Abduction
8	RRingJ1	Right ring	Abs_X: Flexion-Extension Proj_Y: Flexion-Extension Proj_Z: Adduction-Abduction
9	RThirdJ1	Right third	Abs_X: Flexion-Extension Proj_Y: Flexion-Extension Proj_Z: Adduction-Abduction
10	RThumbJ1	Right thumb	Abs_X: Flexion-Extension Proj_Y: Flexion-Extension Proj_Z: Adduction-Abduction
11	RThumbJ2	Right thumb	Abs_X: Flexion-Extension Proj_Y: - Proj_Z: -

Table 4: Anatomical joints' numbers, abbreviations, description of the movements.

Joint	Abbreviation	Description
1	ThumbRotate	Thumb rotation
2	ThumbMPJ	Thumb MCP
3	ThumbIJ	Thumb IP
4	ThumbAb	Thumb Abduction
5	IndexMPJ	Index MCP
6	IndexPIJ	Index PIP
7	MiddleMPJ	Middle MCP
8	MiddlePIJ	Middle PIP
9	MiddleIndexAb	Middle Index Abduction
10	RingMIJ	Ring MCP
11	RingPIJ	Ring PIP
12	RingMiddleAb	Ring Middle Abduction
13	PinkieMPJ	Pinkie MCP
14	PinkiePIJ	Pinkie PIP
15	PinkieRingAb	Pinkie Ring Abduction
16	PalmArch	Palm Arch
17	WristPitch	Wrist Pitch
18	WristYaw	Wrist Yaw

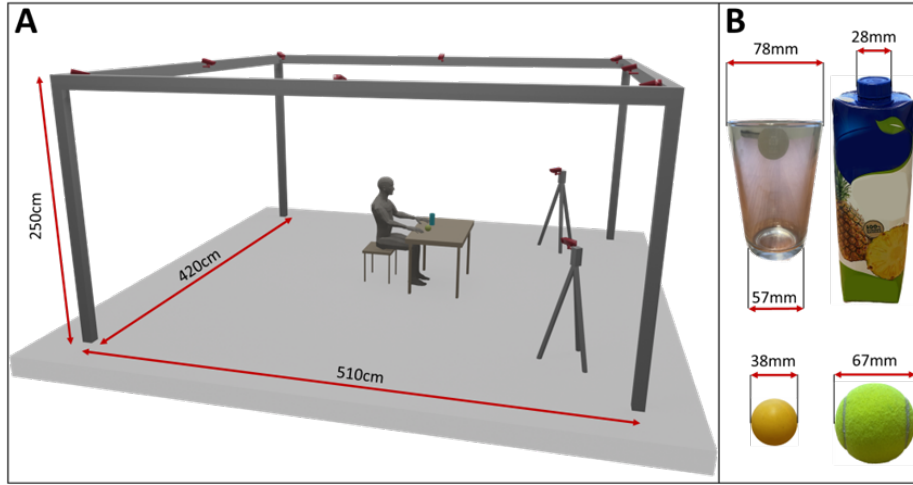


Figure 11: Acquisition environment and grasped objects. A: Representation of the 10 infrared Vicon Cameras (highlighted in red) pointing toward the acquisition volume where the subjects performed the experiment. B: Dimensions of the grasped objects: glass (cylindrical grasp), bottle cap (screw), table tennis ball (tridigital grasp) and tennis ball (spherical grasp).

Table 5: All assigned taxels.

Taxel	Abbreviation	Description	Taxel	Abbr.	Description
1	rmo	RingMiddle	34	ptmd	PalmThumb
2	mdo	MiddleTip	35	tdo	ThumbTip
3	rmi	RingMiddle	36	pcid	PalmWrist
4	mmo	MiddleMiddle	37	imi	IndexMiddle
5	pcim	PalmWrist	38	tmm	ThumbPalm
6	ldd	PinkyTip	39	tdi	ThumbTip
7	rmm	RingMiddle	40	tmi	ThumbPalm
8	rp	RingPalm	41	ptop	PalmThumb
9	rdd	RingTip	42	ptid	PalmThumb
10	lmi	PinkyMiddle	43	ptmp	PalmThumb
11	rdo	RingTip	44	tdm	ThumbTip
12	lmm	PinkyMiddle	45	tdd	ThumbTip
13	lp	PinkyPalm	46	tmo	ThumbPalm
14	rdm	RingTip	47	pcip	PalmWrist
15	ldm	PinkyTip	48	ip	IndexPalm
16	ptip	PalmThumb	49	-	-
17	idi	IndexTip	50	-	-
18	mdi	MiddleTip	51	pcmp	PalmWrist
19	ido	IndexTip	52	-	-
20	mmm	MiddleMiddle	53	-	-
21	ipi	IndexPalm	54	rdi	RingTip
22	mdm	MiddleTip	55	ldi	PinkyTip
23	idd	IndexTip	56	-	-
24	idm	IndexTip	57	lmo	PinkyMiddle
25	imo	IndexMiddle	58	pcmd	PalmWrist
26	pdi	PalmFinger	59	ldo	PinkyTip
27	mmi	MiddleMiddle	60	pdl	PalmFinger
28	pdm	PalmFinger	61	pdr	PalmFinger
29	imm	IndexMiddle	62	pdlo	PalmFinger
30	mdd	MiddleTip	63	lpo	PinkyPalm
31	pdii	PalmFinger	64	-	-
32	mp	MiddlePalm	65	-	-
33	ptod	PalmThumb			

toocol (NTP) synchronized clocks between the Linux and Windows machines. Experimental sessions were video recorded, with data available upon request.

## Data structure

The information was formatted following the Brain Image Data Structure (BIDS) standard<sup>1</sup>, using a dedicated data conversion pipeline. This specialized pipeline systematically arranged the data into a hierarchical filesystem structure aligned with BIDS conventions. An automated process was employed to create folders and files based on the BIDS framework for each participant, as depicted in Figure 4.A.

The data conversion pipeline utilizes the `ft_data2bids` function from Fieldtrip<sup>7</sup>, a Matlab open-source software designed for analyzing electroencephalography. This function was modified to convert the gathered data (depicted as source data in Figure 4.A) into formats compliant with BIDS standards, along with generating the necessary metadata. The pipeline involves a main script that scans a root folder labeled 'source data' and organizes a BIDS compliant data structure based on the subjects and data types found in the source directory. Subsequently, it generates metadata for each data type by invoking a customized version of the `ft_data2bids` function. Since BIDS was initially tailored for neuroimaging data like MEG and EEG, adjustments were made to `ft_data2bids` to accommodate our specific data types: EMG, motion, and tactile data. Each data type was transformed into a BIDS-compliant format in accordance with the provisional guidelines outlined by the BIDS community working groups.

Because the source data is extensive, we've opted to share only the raw BIDS compliant dataset. Therefore, the code utilized to convert the source data into BIDS compliant raw data will be provided upon request.

The central directory, labeled as 'haptic\_object\_exploration' in Figure 4.B, comprises BIDS compliant folders for each subject, accompanied by their metadata. Each subject's folder is denoted as `sub-XX`, where `XX` represents the subject number (e.g., `sub-01`, `sub-02`, ..., `sub-11`). Within each subject's folder, there exist three subfolders named `emg`, `motion`, and `tactile`, dedicated to EMG, kinematic, and touch data, respectively (see Figure 4.B). Each of these folders contains three distinct files corresponding to the 45 conditions: a `.csv` file containing raw data, a `.json` file containing metadata specific to the recording modality, and a `.tsv` file containing channel descriptions.

File naming conventions dictate that `.csv` and `.json` files follow a specific format: they are named as `sub-XX_task-GIVEN_SPOKEN_acq-ZZ_FF`. Here, `XX` represents the subject number, `GIVEN_SPOKEN` denotes the handed over and named object, `ZZ` signifies the acquisition system (like `cometa` or `sessantaquattro` for EMG data, `vicon` or `cyberglove` for kinematic data, and `tactileglove` for touch data), and `FF` indicates the containing folder, corresponding to the data type (such as `emg`, `motion`, and `tactile`).

The `.tsv` file is titled `sub-XX_task-GIVEN_SPOKEN_acq-ZZ_channels`, dif-

fering from other files by replacing the folder name (FF) with the suffix "channels". In the .csv file, the first column holds timestamps, while subsequent columns hold individual channel data. This file lacks a header, but the channel names are listed in the .tsv file in the same sequence. Additional details can be found in Supplementary Table 6 within the .tsv file.

Metadata is stored within the .json files, offering various details as outlined in Supplementary Table 7.

## Data repository

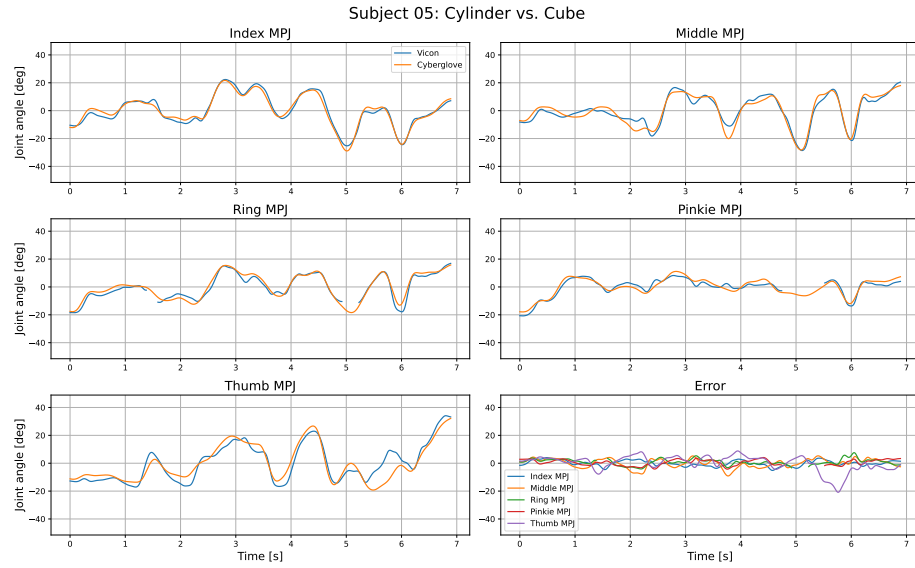
The IIT Dataverse, managed by the Istituto Italiano di Tecnologia, serves as the institution's repository for research data. It utilizes the Dataverse software, originally developed at Harvard University, and assigns persistent DOIs to uploaded data for easy retrieval. Accessible via HTTPS protocol, it is indexed in OpenAIRE Explore and registered in re3data.org. The platform offers APIs, including a SWORD API, for dataset search and access. Data uploads include citation metadata, customizable domain-specific metadata, and file-level metadata. Metadata can be exported in various standard formats for interoperability. Dataverse supports open licenses such as Creative Commons and allows customization of data usage agreements. Managed by the IIT Research Data Management service, the platform ensures dataset quality and FAIRness (Findable, Accessible, Interoperable, and Reusable) through basic data curation.

## 3 Technical Validation

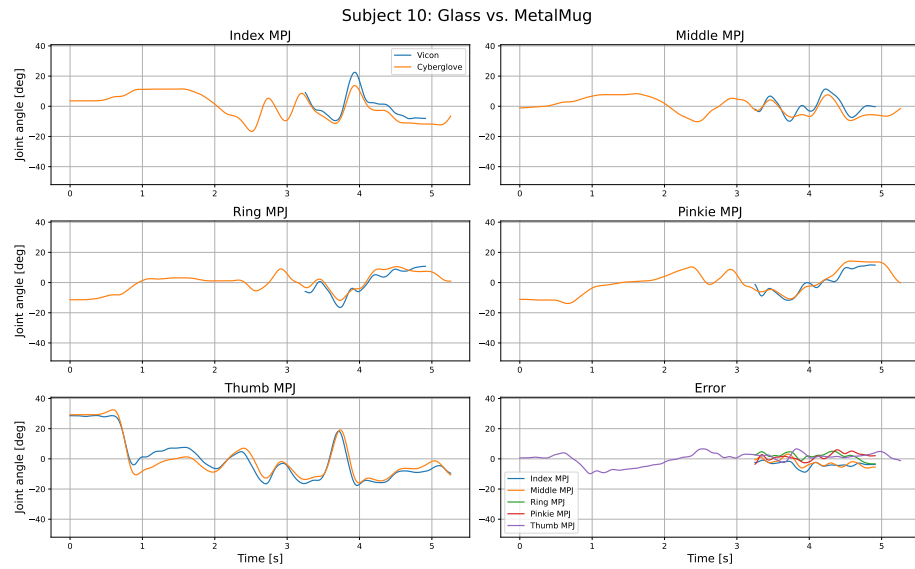
### 3.1 Kinematic data

The data gathered by the CyberGlove must be subject specifically tuned for each joint to accommodate for different hand sizes. To do so the data from the optical tracking (Vicon system) was used as ground truth. Every joint ( $n$ ) has its offset  $\mu$  and scale  $\alpha$ . By minimizing the error between the joint trajectories over all trials per subject ( $S$ )  $\mu_n(S)$  and  $\alpha_n(S)$  are derived. The optical tracking covers only the first joint of each finger, the MPJ. The MPJ and PIJ can be treated as a coupled system with similar properties allowing to apply the same scale ( $\alpha_n(S)$ ) found for the MPJ. Data from the optical tracking has partly missing data points due to self occlusion due to hand rotation, but covers next to the hand the kinematics of the right arm and the upper body.

The kinematic data carries task dependent information. Comparing data within an object family reveals, that objects similar in size and shape have similar distribution in the joint space, like Fig. ?? settle differences for the drinking vessels vs notably differences for the balls.



(a) Data from optical tracking used to tune the CyberGlove traces.



(b) Missing data points in optical tracking due to occlusion.

Figure 12: Matching the CyberGlove using the data from the optical tracking.

## EMG data

To verify the quality of the EMG data for both bipolar and high-density signals, we performed a frequency analysis. Since the spectrum of the EMG signals



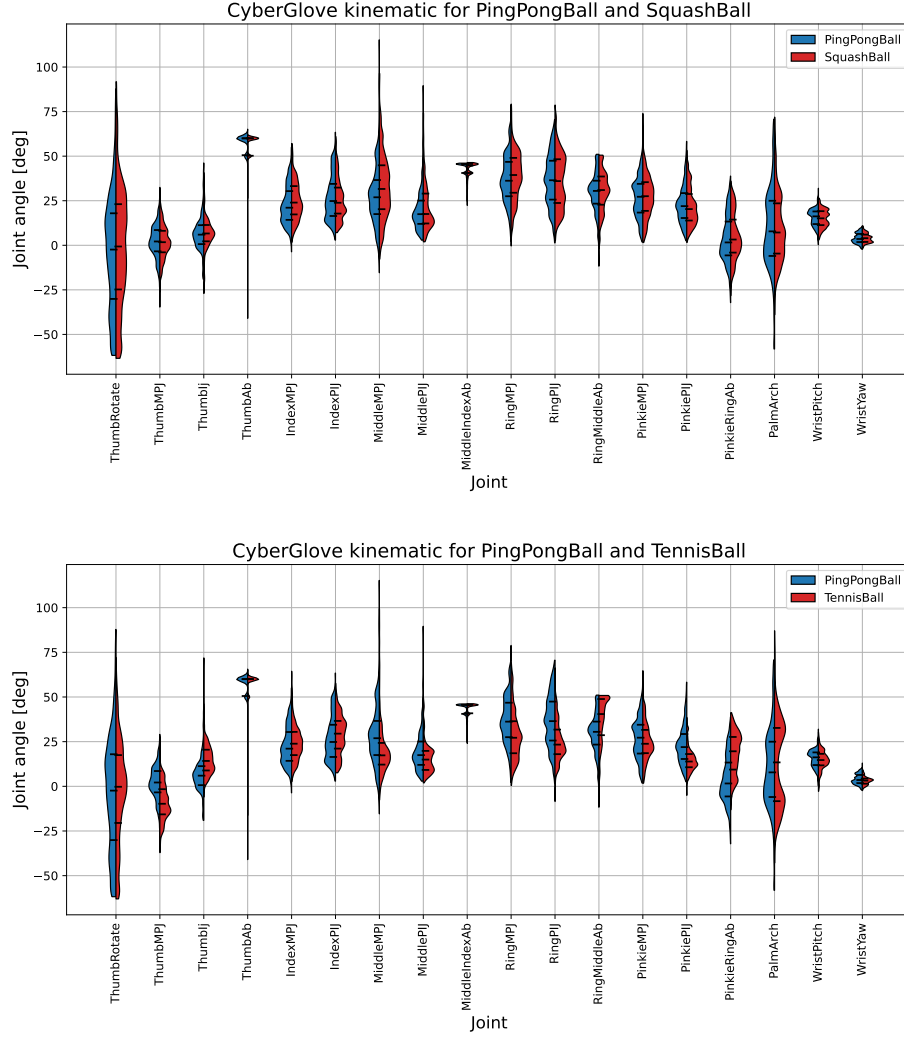


Figure 13: Matching the CyberGlove using the data from the optical tracking.

ranges between 10Hz and 500Hz[9], we first applied a 4th order bandpass filter (cut-off frequencies: 10Hz and 500Hz), we then used a 6th bandstop filter (cut-off frequency: 50Hz) to attenuate the power-line interference. After filtering the EMG data, we computed Power Spectral Density (PSD) via the Welch's method[10], to estimate the spectrum of the acquired signals. The PSD for the HD-sEMG and bipolar EMG are graphically represented in Figure 5.A and Figure 5.B, respectively.

shows mean and median

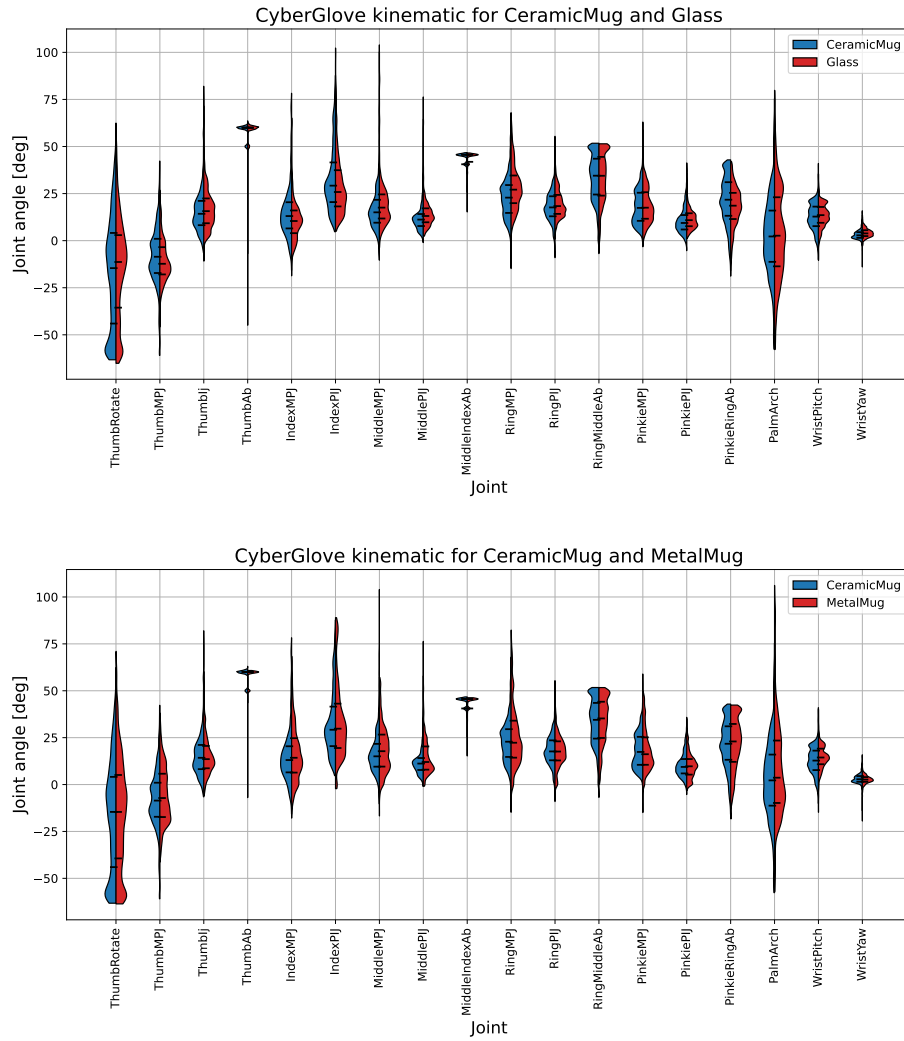


Figure 14: Matching the CyberGlove using the data from the optical tracking.

## Tactile data

## Exploratory procedures

## References

- [1] Andrea Leo et al. “A synergy-based hand control is encoded in human motor cortical areas”. In: *Elife* 5 (2016), e13420.

Table 6: Exploratory procedures labels and description.

Name	Description
Contour following	Following along an edge with a single digit.
Enclosure	Wrapping the finger around the full object.
Enclosure part	Pinching a part of the object between the fingers.
Function test	Extracting part function.
Pressure	Squeezing the object.
Rotation	Turn the object along single axis.
Translation	Move the object linearly along single axis.
Weighting	Periodic handmovement driven by the elbow.

- [2] Alessandro Scano et al. “Muscle synergy analysis of a hand-grasp dataset: a limited subset of motor modules may underlie a large variety of grasps”. In: *Frontiers in neurorobotics* 12 (2018), p. 57.
- [3] Nikolai Aleksandrovich Bernstein. *The control and regulation of movements*. London: Pergamon Press, 1967.
- [4] Michael T. Turvey. “Action and perception at the level of synergies”. In: *Human movement science* 26.4 (2007), pp. 657–697.
- [5] Pramodsingh H. Thakur, Amy J. Bastian, and Steven S. Hsiao. “Multi-digit movement synergies of the human hand in an unconstrained haptic exploration task”. In: *Journal of Neuroscience* 28.6 (2008), pp. 1271–1281.
- [6] Reinhard Gentner and Joseph Classen. “Modular organization of finger movements by the human central nervous system”. In: *Neuron* 52.4 (2006), pp. 731–742.
- [7] Verónica Gracia-Ibáñez et al. “Sharing of hand kinematic synergies across subjects in daily living activities”. In: *Scientific reports* 10.1 (2020), pp. 1–11.
- [8] Susan J. Lederman and Roberta L. Klatzky. “Hand movements: A window into haptic object recognition”. In: *Cognitive psychology* 19.3 (1987), pp. 342–368.
- [9] Susan J. Lederman and Roberta L. Klatzky. “Extracting object properties through haptic exploration”. In: *Acta psychologica* 84.1 (1993), pp. 29–40.
- [10] Ahmed Fawzy Gad. “Pygad: An intuitive genetic algorithm python library”. In: *Multimedia Tools and Applications* (2023), pp. 1–14.

Exploratory procedures per task

	Balls	Cutlery	Drinking vessels	Geometric objects	Plates
Contour following	0 3 0 0 0 0 4 4 4 2	2 2 1 4 2 3 7 4 1 1	1 2 1 2 0 3 2 0 1	4 3 4 3 3 3 2 4 4	1 3 1 3 3 4 1 1
Enclosure	10 10 9 9 8 10 10 10 10 10	10 10 10 9 9 10 10 10 10 10	7 7 7 10 10 9 7 6 5	11 9 12 9 12 10 9 8 6	10 10 9 11 10 9 10 10 10
Enclosure part	0 1 0 0 0 0 1 1 1 1	3 3 4 1 1 3 4 5 7 7	10 10 12 8 8 9 8 8 5	5 5 7 3 2 4 1 1 1	0 0 0 3 0 0 0 0 0
Function test	0 0 0 0 0 0 0 0 0 0	7 8 1 7 4 4 1 0 0	0 0 0 0 0 0 4 1 4	0 0 0 0 0 0 0 0 0	0 0 0 0 0 0 0 0 0
Pressure	13 18 12 11 15 14 9 10 11	0 0 0 1 0 0 0 0 0	0 0 0 0 0 0 0 0 0	0 0 0 0 0 0 1 0 1	0 0 0 3 3 2 4 0 0
Rotation	0 4 1 0 1 0 1 2 2 2	4 1 4 3 2 3 3 5 6 6	0 0 0 0 0 0 0 0 0	0 0 0 0 0 0 0 0 0	0 0 0 1 1 1 0 0 0
Translation	12 9 7 4 6 1 2 1 1 1	7 7 6 10 11 10 6 7 4 4	0 0 0 0 0 0 2 0 3	0 0 0 0 0 0 0 0 0	0 0 0 0 0 0 0 0 0
Weighting	0 0 0 0 0 0 0 0 0 0	0 0 0 0 0 0 0 0 0	1 1 2 2 2 2 3 2 2	0 0 0 0 0 0 0 0 0	0 0 0 0 0 0 0 0 1
Total	37 45 39 24 31 28 26 28 27 27	31 29 32 35 36 38 31 29 32 32	27 36 38 33 26 27 28 26 30 30	27 21 32 28 26 22 22 20 20 20	9 8 5 10 10 6 1 0 0 1
	PingPongBall_PingPongBall	Fork_Fork	CeramicMug_CeramicMug	Cube_Cube	CeramicPlate_CeramicPlate
	PingPongBall_SquashBall	Fork_Knife	CeramicMug_Glass	Cube_Cylinder	CeramicPlate_MetalPlate
	PingPongBall_TennisBall	Fork_Spoon	CeramicMug_MetalMug	Cylinder_Cube	CeramicPlate_PlasticPlate
	SquashBall_PingPongBall	Knife_Fork	Glass_CeramicMug	Cylinder_Cylinder	MetalPlate_CeramicPlate
	SquashBall_SquashBall	Knife_Knife	Glass_Glass	Triangle_Cube	MetalPlate_MetalPlate
	SquashBall_TennisBall	Spoon_Fork	Glass_MetalMug	Triangle_Cylinder	MetalPlate_PlasticPlate
	TennisBall_PingPongBall	Spoon_Knife	MetalMug_CeramicMug	Triangle_Triangle	PlasticPlate_CeramicPlate
	TennisBall_SquashBall	Spoon_Spoon	MetalMug_Glass		PlasticPlate_MetalPlate
	TennisBall_TennisBall		MetalMug_MetalMug		PlasticPlate_PlasticPlate
					Total
					126 422 164 122 162 110 147 162 124 59

Accuracy per task

	Balls	Cutlery	Drinking vessels	Geometric objects	Plates
Sub-01					
Sub-02					
Sub-03					
Sub-04					
Sub-05					
Sub-06					
Sub-07					
Sub-08					
Sub-10					
Sub-11					
Total	0.90 0.80 0.90 0.90 0.80 0.80 0.70 0.70 0.80 0.80 0.80 1.00 0.97				
	PingPongBall_PingPongBall				
	PingPongBall_SquashBall				
	PingPongBall_TennisBall				
	SquashBall_PingPongBall				
	SquashBall_SquashBall				
	SquashBall_TennisBall				
	TennisBall_PingPongBall				
	TennisBall_SquashBall				
	TennisBall_TennisBall				
	Fork_Fork				
	Fork_Knife				
	Fork_Spoon				
	Knife_Fork				
	Knife_Knife				
	Knife_Spoon				
	Spoon_Fork				
	Spoon_Knife				
	Spoon_Spoon				
	CeramicMug_CeramicMug				
	CeramicMug_Glass				
	CeramicMug_MetalMug				
	Glass_CeramicMug				
	Glass_Glass				
	Glass_MetalMug				
	MetalMug_CeramicMug				
	MetalMug_Glass				
	MetalMug_MetalMug				
	Cube_Cube				
	Cube_Cylinder				
	Cylinder_Cube				
	Cylinder_Cylinder				
	Cylinder_Triangle				
	Triangle_Cube				
	Triangle_Cylinder				
	Triangle_Triangle				
	CeramicPlate_CeramicPlate				
	CeramicPlate_MetalPlate				
	CeramicPlate_PlasticPlate				
	MetalPlate_CeramicPlate				
	MetalPlate_MetalPlate				
	MetalPlate_PlasticPlate				
	PlasticPlate_CeramicPlate				
	PlasticPlate_MetalPlate				
	PlasticPlate_PlasticPlate				
	Total				

(a) Accuracy per task, object family and (b) Exploratory procedures per task and object group.

EPs per subject

Contour following	7	8	17	10	18	12	16	8	10	14	120
Enclosure	45	40	43	45	44	36	42	41	45	41	422
Enclosure part	19	19	16	19	20	14	7	20	24	6	164
Function test	10	6	7	4	12	6	9	4	13	1	72
Pressure	17	21	9	12	23	8	10	8	19	15	142
Rotation	18	17	8	13	26	3	18	9	24	11	147
Translation	18	15	14	9	15	10	12	12	22	1	128
Weighting	6	5	8	6	5	4	6	7	6	6	59
Total	140	131	122	118	163	93	120	109	163	95	1254
	sub-01	sub-02	sub-03	sub-04	sub-05	sub-06	sub-07	sub-08	sub-10	sub-11	Total

Figure 16: Exploratory procedures used by name and subject.

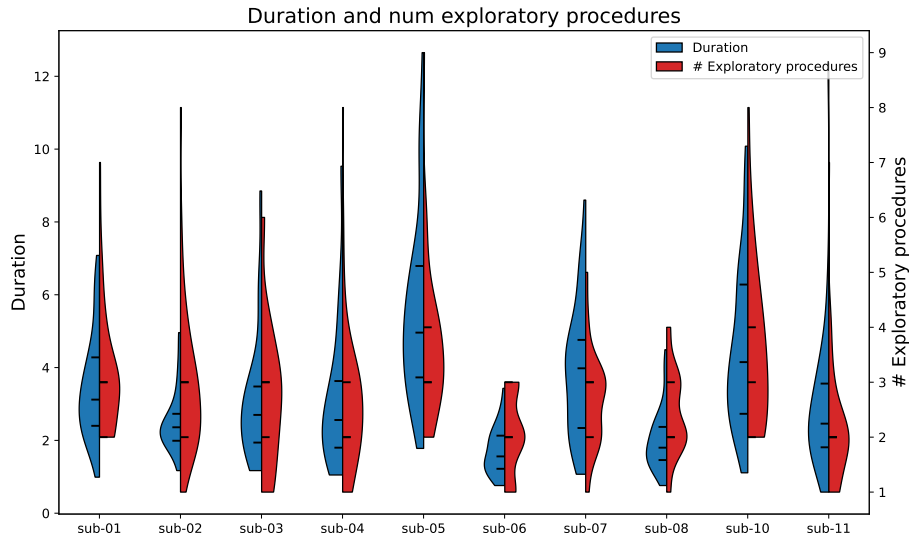


Figure 17: Exploration time and number of exploratory procedures per subject per task.